REPORT DOCUMENTATION PAGE		READ INSTRUCTIONS BEFORE COMPLETING FORM
1. REPORT NUMBER AFAL-TR-74-320	2. GOVT ACCESSION NO.	3. RECIPIENT'S CATALOG NUMBER
4. TITLE (and Subtitle) LOW-RCS VEHICLE STUDY (U)		5. TYPE OF REPORT & PERIOD COVERED Technical Report, Final 11 January 1973 - 1 May 1974
		6. PERFORMING ORG. REPORT NUMBER TRA 29369-4A
7. AUTHOR(s) H. W. Lorber, PhD R. W. Wintersdorff G. R. Cota		8. CONTRACT OR GRANT NUMBER(s) F33615-73-C-1217
9. PERFORMING ORGANIZATION NAME AND ADDRESS Teledyne Ryan Aeronautical 2701 Harbor Drive San Diego, California 92112		10. PROGRAM ELEMENT, PROJECT, TASK AREA & WORK UNIT NUMBERS 62204F/7633/03/19
11. CONTROLLING OFFICE NAME AND ADDRESS Air Force Avionics Laboratory/WRP Wright-Patterson AFB, Ohio 45433		12. REPORT DATE 31 January 1975
		13. NUMBER OF PAGES 66
14. MONITORING AGENCY NAME & ADDRESS(If different from Controlling Office)		15. SECURITY CLASS. (of this report) SECRET
		15a. DECLASSIFICATION/DOWNGRADING SCHEDULE Exempt (Category 3) Ind.

[handwritten: this document has had classified portions removed. Lynn Kane FOIA Assistant 8/12/2002]

16. DISTRIBUTION STATEMENT (of this Report)

Distribution limited to U. S. Government agencies only:
Covers the test and evaluation of military hardware; 31 January 1975. Other
requests for this document must be referred to AFAL/WRP.

17. DISTRIBUTION STATEMENT (of the abstract entered in Block 20, if different from Report)

18. SUPPLEMENTARY NOTES

This work has been partially supported by Air Force Avionics Laboratory Director's
Discretionary Funds (LDF73-164).

19. KEY WORDS (Continue on reverse side if necessary and identify by block number)

Radar camouflage	Pilotless aircraft
Radar cross sections	Radar countermeasures
Reconnaissance drone aircraft	

20. ABSTRACT (Continue on reverse side if necessary and identify by block number)

See reverse side.

(U) On the basis of theoretical insights generated during the current study, very high payoff is anticipated from a relatively small follow-on study of edge-treatment design theory and fabrication. Further edge-treatment work is also indicated in areas of computer simulation, experimental measurement, and materials.

FOREWORD

GLOSSARY

A-band	0 - 250 MHz
Anti-Radar Performance	A popular term roughly synonymous with the reciprocal of the radar cross-section
Attenuation	Reduction in strength or power
Backscatter	Reradiation of incident radar energy back toward the radar
B-band	250 - 500 MHz
Broadside	Any direction perpendicular to the direction along a metal edge or edge treatment
Bulk Dielectric or Bulk Absorber	Occupying an appreciable volume, in particular as opposed to thin-sheet dielectric or thin-sheet absorber
dB	Decibels - A real number equal to $10 \log_{10} x$, where x is a positive number, usually the ratio of two power levels
dBsm	Decibels referred to one square meter - A real number equal to $10 \log_{10} \sigma$, where σ is an area, such as a radar cross-section, expressed in square meters
Edge Treatment	A strip of radar absorbing material attached to a metal edge to reduce its backscatter
E-polarization	Electric field oriented parallel to an edge
GHz	Gigahertz - A unit of frequency equal to 1000 megahertz
H-polarization	Magnetic field oriented parallel to an edge
Length	When used in connection with edge treatment, the linear extent of an edge treatment in the direction along the treated metal edge

(U)

GLOSSARY (Continued)

MHz	Megahertz – A unit of frequency equal to 1 million hertz (A hertz is a complete reversal of the direction of an current, voltage, or velocity, and its return to its original direction in one second.)
Outflanking	When used with reference to edge treatment, an effect whereby radar waves incident on a horizontal treated metal edge bypass the edge treatment above and below and make their way to and from the metal edge largely unattenuated
Radar Reflectivity	A popular term roughly synonymous with radar cross-section
RAM	Radar absorbing material
RCS	Radar Cross-Section – A measure of the ability of a target, such as an aircraft, to reradiate the power transmitted by a radar back to the radar in a form that the radar receiving antenna can utilize (The RCS is expressed in units of area – synonym: echo area.)
RPV	Remotely Piloted Vehicle – An aircraft controlled from a remote location
Thickness	When used in connection with edge treatment, the linear extent of an edge treatment in the direction perpendicular to its width
TRA	Teledyne Ryan Aeronautical
Width	When used in connection with edge treatment, the distance from the outboard to the inboard edges of an edge treatment

(II)

(U) The Low-RCS* Technology Program (Model 237) allowed the Air Force to explore a potentially important technology which had been closely held by Teledyne Ryan Aeronautical (TRA). When the program was cancelled, for lack of a requirement of combat, the Observables Group of the Air Force Avionics Laboratory (AFAL) secured sufficient Laboratory Director's funds to continue the RCS portion of the program. The general purpose of the present study, which is that continued effort, was to go beyond the very preliminary measurements and calculations of the prior work to demonstrate and evaluate potential of this technology for Air Force application.

(U) The purpose of radar camouflage is to deny to the enemy:

      a.   Detection of our aircraft

      b.   Tracking of our aircraft

      c.   Fuzing of his missiles launched against our aircraft

(U) Detection - Denying to the enemy his ability to detect our aircraft gives us the ability to deliver weapons with complete surprise and to penetrate his airspace covertly to conduct reconnaissance. Moreover, denial of radar detection prevents his commitment of manned intercepters. Denial of detection requires camouflage across the entire threat radar spectrum (Figure 2). Moreover, the radar reflectivity of our aircraft must be somewhate less than some threshold level in order to be at all effective. Naturally, the usual radar countermeasures such as chaff (myriad, small, light, radar reflectors dispensed into the slipstream of an aircraft) and jamming cannot be used in this application.

(U) Tracking - Denying to the enemy his ability to track our aircraft with radar greatly increases our ability to penetrate his airspace overtly. Denial of tracking requires camouflage only across the microwave spectrum. Moreover, chaff and active electronic countermeasures are useful in this application and any reduction in the radar reflectivity of our aircraft improves the effectiveness of these countermeasures.

(U) Fuzing - Reducing the reflectivity of our aircraft at the frequencies of threat radar proximity fuzes becomes very effective when radar camouflage reduces the maximum fuzing distance of threat weapons to roughly 40 percent or less of their CEP (Figure 3).

(U) Effect of Altitude on Detectability - The higher an aircraft flies, the farther it is from a radar on the ground (obviously). More importantly, since the RCS level necessary to escape detection varies as the fourth power of the distance from the radar to the aircraft, it also varies as the fourth power of the altitude of the aircraft ($\sigma_{undetectable} \propto h^4$). This relationship is exhibited in Figure 2. Thus, an aircraft that is quite detectable at one altitude can become undetectable by climbing to a somewhat higher altitude.

(U) * The radar reflectivity of an aircraft is measured in terms of its radar cross-section (RCS), a quantity usually expressed in square meters (sq. m or m^2) and denoted mathematically by a lower case Greek sigma (σ).

(U)   Effect of Chaff and Jamming on Tracking - Manual tracking may still be available to an enemy with a vehicle dispensing chaff, but not automatic tracking. A tracking radar needs a high degree of angular and range resolution or moving target indication (MTI) in order to combat chaff. For "self screening", in which an aircraft uses chaff or jamming to "break track" of a tracking radar on itself, the number of pounds of chaff and the number of watts of jamming power necessary to break track are directly proportional to the RCS of the aircraft. Thus, reducing the RCS of an aircraft by a factor of 9 reduces the necessary chaff load or jammer power by a factor of 9, also. Moreover, for an aircraft with a jammer flying toward a radar, reducing the aircraft RCS by a factor of 9, and retaining the same jammer power, reduces by a factor of 3 the range at which the radar echo of the aircraft "burns through" the screen of noise generated by the jammer. This reduces the ground surface area over which the aircraft must do without jammer protection by a factor of 9.

(U)   Further Advantages of Low-Vehicle RCS - Radar camouflage, as exemplified by the aircraft discussed in Section 2.0 and 4.0 of the present report, defeats any advantage the enemy may try to gain through the introduction of sophisticated "electronic counter-countermeasures" (ECCM) such as frequency agility, variable pulse repetition rates, and noise modulation. Moreover, MTI, which is effective against chaff, as mentioned above, is of no use in improving the detectibility of a low-RCS aircraft.
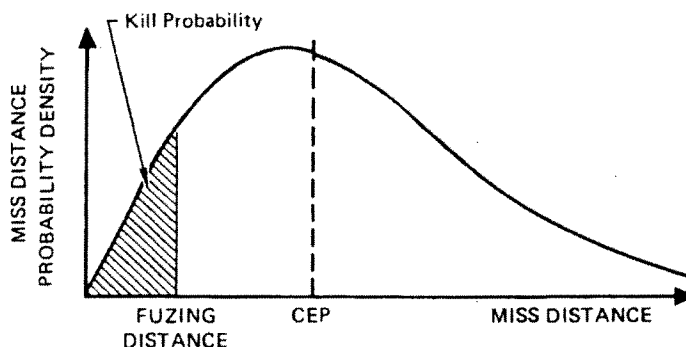
(U)   Figure 3. Illustrating the Small Kill Probability (0.105) That Results From a Fuzing Distance Equal to 40 Percent of the CEP. (Area Under the Entire Curve Equals 1.00)

(U)   Feasibility Tests - Testing philosophy was to measure the RCS of the model described above, in a series of demonstration tests. To aid in the analysis of data from these tests, diagnostic tests were also run.

(U)   Validity of demonstration test results was ensured by a thorough program of error identification and repetition of tests.

(U) The vehicle is an embodiment of an innovative design concept incorporating attention to electrodynamic as well as aerodynamic principles.*

(U) The basic philosophy embodied by the vehicle is one of efficient aerodynamic design, with a minimum number of radar scatterers of minimum strength or effectiveness. Thus, the Low-RCS Demonstration Vehicle is quite simple in form; it has no fuselage, no tail, and no nacelles. See Figure 6.

(U) Model Configurations - Consider the 1/3-scale RCS model as consisting of a featureless centerbody designated as A, let us say; an edge treatment B; and four individual localized features: the engine inlet C_1, engine exhaust duct C_2, elevons C_3, and vertical stabilizers, C_4. Demonstration tests were run with the model Configuration $ABC_1C_2C_3C_4$. Diagnostic tests were run on a "base configuration" AB of minimum RCS and on other configurations that differed from the base configuration by only one modification, e.g., A, ABC_3, ABC_4. Configurations ABC_2, ABC_3, and ABC_4 were tested only at zero degrees of roll.

(U) Test Range Geometry - The test data suggest a straight and level fly-by, over a flat earth, past a ground-based radar, as shown in Figure 7. The model was mounted on the test range as shown in Figure 8 on the facing page. The view shown is that seen from the test-range radar. With reference to the fly-by situation, it is apparent that a 180-degree range of azimuth is all that is necessary. The other 180 degrees are superfluous. The model was mounted inverted so that reflections from radar-to-model-to-ground-to-model-to-radar would be minimized during the necessary 180-degree interval.

(U) Data Presentation - Test data are presented graphically as plots of RCS as a function of azimuth, over the necessary 180-degree interval, in polar form, with frequency, polarization, and roll angle as parameters.

(U) Roll angles used in the tests were 0, 10, 20, 30, 40, and 50 degrees.

(U) Polarizations used by the test-range radar were horizontal (HH) and vertical (VV) with respect to the test-range ground plane. These polarizations are representative of the polarizations of a conical-scanning radar on the ground trying to track the low-RCS vehicle flying by.

(U) Data Presented - The complete data set of 48 semicicular azimuth plots could have been presented as six frequency foldouts or eight roll-angle foldouts, but either choice would have resulted in excessive data presented, in comparison with the amount of useful information available there. Consequently, the two foldouts of Figures 9 and 11 were chosen as being representative and presenting most clearly the variations of RCS with frequency, roll-angle and polarization.

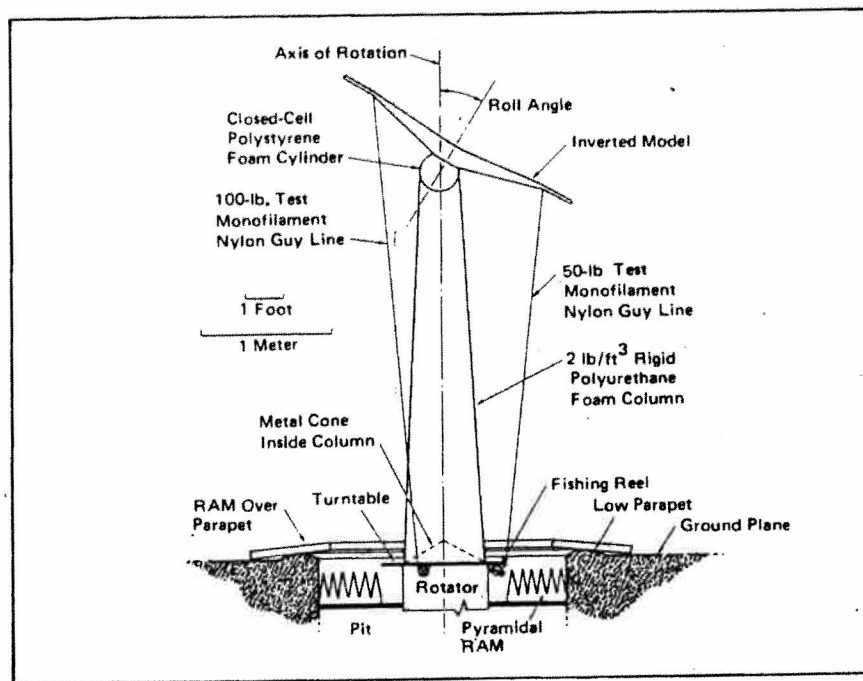*Patent applied for: Application No. SN465,540.

Figure 8. Model Mounting Arrangement on Ground-Plane Test Range

(U)

(U) Analysis: Roll Angle - The 1.57 GHz results presented in the opposite foldout are typical of the variation of RCS with roll angle at frequencies of 900 MHz and above.

(U) An elementary analysis of the reflection that would be produced by the longitudinal interface between dielectric layers in the edge treatment was able to account for the observed backscatter with only a 4-dB error. But this analysis was based on the assumption of an electric field of uniform magnitude over the entire surface of the interface. A calculation of the field distribution in a small neighborhood of the vertex of the wedge-shaped interface indicated that the uniform-field assumption was approximately correct. Thus, the assumption of a simple reflection from the interface was able to account for the strength of the observed backscatter and was consistent with the field distribution required at the vertex of the interface by the form of the Maxwell field equations.

(U) Low-RCS Demonstration Vehicle: 1/3-Scale Model - The 1/3-scale model was designed so that ideally its RCS would scale to that of the demonstration vehicle at all aspects. Moreover, the model was made demountable so that it could be reconfigured in the field for diagnostic as well as demonstration tests. Model design features are detailed below, together with comments on how they affected test data.

(U) Polystyrene foam mounting block. This prominent feature in Figures 8 and 17 was fastened to the model with a thin, but irregularly surfaced epoxy layer. Effect on data: The exposed surfaces of the block have been suspected of causing spurious reflections, but have been exonerated in each specific instance. The epoxy layer may have a bad effect at vertical polarization, at zero and 10 degrees roll, at the highest frequencies, and at all azimuths. Backscatter of this generality in azimuth is very difficult to discern in the data. Consequently, in the presence of numerous other artifacts in the data, no specific data features have been attributed to the epoxy layer.

(U) Monofilament guy lines. Monafilament nylon fishing line was used to guy the model. The guy lines were fastened to the model at the three vertices in tiedown fixtures that were buried inside the model. Effect on data: Backscatter from the guy lines themselves was prominent in the data but was quite localized* and easily identified. The tiedowns' contributions were negligible.

(U) Test-Range Considerations - Ideally, the test-range radar illuminates and observes the 1/3-scale model uniformly and responds only to backscatter from the model itself. In actuality, the model was illuminated and observed with some nonuniformity over the model, and at all test frequencies some energy found its way into the radar receiver from sources other than the model itself. This additional energy was responsible for a positive "background level" against which the model was measured, and it limited the accuracy with which the RCS of the model could be measured.

(U) On the opposite page, background level is tabulated for each frequency, together with a measure of the uniformity of illumination and observation. The background level is expressed in square meters (m^2) and in decibels above one square meter (dBsm). That is, the background level is expressed in terms of the RCS of a radar target that would backscatter an equivalent amount of energy into the test-range receiving and recording system. The uniformity of illumination and observation (called simply 2-way illumination in the table notes) is expressed in decibels of maximum deviation over a rectangular field.

(U) The background level of the test range consisted of two parts: direct feedthrough of the decaying trailing edge of the transmitter pulse into the receiver (an especially serious problem at the two lowest frequencies) and backscatter from the rigid polyurethane foam column used to support the model. Both sources of background have been lumped together in the tabulated background level figures.

(U) Backscatter from a foam support column consists of two components. One component, is known as "coherent" backscatter, due to the spatially averaged dielectric constant of the column material being greater than that of air. The other, due to random nonhomogeneities in the foam material, is known as "incoherent" backscatter. The test frequencies from 273 MHz on up were chosen to minimize coherent backscatter. Incoherent backscatter was not amenable to frequency selection.

(U) * An elementary calculation shows that the RCS of a guy line is no more than one percent of its maximum value, at the highest test frequencies, at angles more than a few degrees from the backscatter peak.

(U) Significance of the background level is this: when the background backscatter is 20 dB below (1 percent of) the model RCS, the measured RCS may be 1 dB (26 percent) in error. When the background is 10 dB below (10 percent of) the model RCS, the measured RCS may be 3 dB (100 percent) in error. These values are sufficient to provide a rough assessment of the accuracy of data presented in Figures 9 and 11. For greater detail in the relationship between background level and data error, see Figure 23.

TABLE 3

BACKGROUND LEVEL[a] AND ILLUMINATION FLATNESS[b]

FREQUENCY (GHz)	BACKGROUND LEVEL		FLATNESS (dB)
	(m^2)	(dBsm)	
0.100	0.006	-22	2.4
0.167	0.004	-24	1.0
0.273	0.0008	-31	0.7
0.900	0.0002	-36	0.5
1.57	0.0004	-34	0.5
3.33	0.0004	-34[c]	0.6
3.50	0.0006	-32[c]	0.9
8.00	0.002	-27[c]	0.7

NOTES: (a)   Absolute maximum values.

(b)   Maximum absolute deviation from the 2-way illumination level at the center of a field 4 feet high by 10 feet wide.

(c)   Occasional incoherent spikes. Average value less than -46 dBsm $(0.00003 \ m^2)$.

(U)

(U) Four edge-treatment engineering techniques were used in the optimization effort. None of these techniques are original with Teledyne Ryan Aeroanutical (TRA), but all of them have been developed further in the course of the present program. They are the following:

- Edge-treatment characterization. Quantitative standards facilitated the applicability of two-dimensional edge-scattering theory to the radar camouflage of three-dimensional aircraft.

- Computer simulation. Special subroutines improved the efficiency of existing programs for engineering design by at least order of magnitude.

- Experimental measurement. Special techniques facilitated the trial of many candidate edge treatments at minimum expense.

- Physical realization. Special techniques were developed for the actual fabrication of theoretical designs.

(U) One and two-dimensional (1-D and 2-D) scattering concepts help greatly to simplify the development of radar camouflage for practical three-dimensional (3-D) aircraft. Ordinary mirror-like reflection is inherently a 1-D process, whereas edge scattering is inherently 2-D. Accordingly, on these pages we compare and contrast the very well known 1-D characterization of reflection camouflage with the less familiar 2-D characterization of edge camouflage.

(U) 1-D: Mirror-Like Reflection - The applicability of the 1-D characterization for backscattering is limited to flat and gently-curved surfaces at least a few wavelengths in "diameter" (i.e., surfaces having principal radii of curvature large compared to a wavelength and having edges at least a wavelength away from the geometrical-optical point of reflection).

(U) 1-D characterization is in terms of a reflection coefficient R, a real positive number, usually no greater than 1. The reflection coefficient is a function of the frequency and polarization of the (monostatic) radar.

(U) 3-D application to radar camouflage is in terms of the equation $\sigma = R\sigma_0$, where σ is the radar cross-section (RCS) of that portion of the camouflaged aircraft undergoing reflection and σ_0 is the corresponding RCS that would exist if the reflecting surface were a perfect, or nearly perfect, metal conductor. Ideally, $R = 0$. The worst case is $R = 1$. In typical aircraft camouflage applications, one often encounters panels of radar absorbing material (RAM) having R equal to 0.05 (-13 dB) or less.
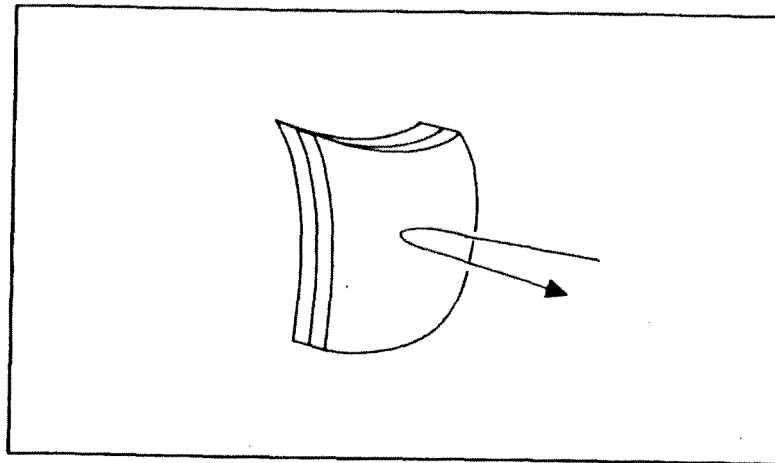
Figure 19. Reflection from a Gently-Curved, Layered Panel of Radar
Absorbing Material (RAM)

(U) 2-D: Edge Backscatter - The applicability of the 2-D characterization for backscattering
from edges is limited to straight and gently curved edges at least a few wavelengths long
(i.e., surfaces having one principal radius of curvature large compared to a wavelength
and one small, and having edges at least a wavelength away from the point of backscatter,
as defined in accordance with the Geometrical Theory of Diffraction).

(U) 2-D characterization is in terms of a normalized RCS, B, a real positive number equal
to the RCS of a straight edge of unit length, in the absence of finite-length effects, at
any aspect broadside to the edge*. Thus, the normalized RCS is a function of the fre-
quency and polarization of the (monostatic) radar as well as the aspect angle at which it
views the edge. (In the general 3-D characterization, aspect would have to be expressed
in terms of a pair of angles.) The edge can face toward or away from the radar; the
characterization is valid in either case.
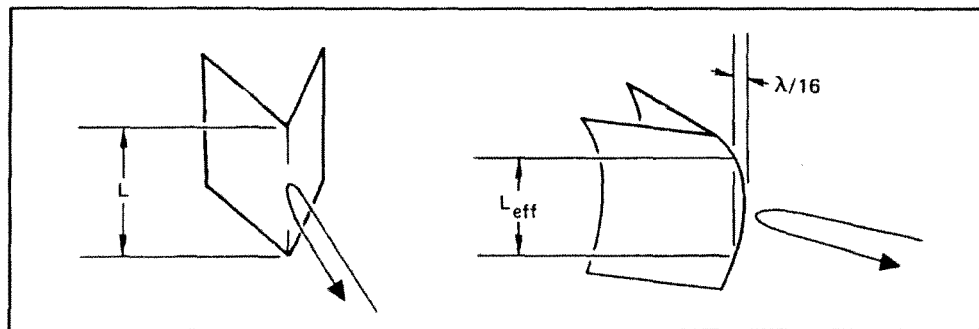
(U)   Figure 20. Backscattering from a Straight Edge of Length L, and from a Curved
Edge of Effective Length L_{eff}. Here, λ is the Radar Wavelength

(U) * A two-dimensional RCS σ_{2D}, expressed in units of length, is often used in the
theoretical literature on 2-D scattering. The 2-D RCS is avoided here because B
is more directly applicable to 3-D camouflage. A convenient conversion formula
is $B = \sigma/L^2 = 2\sigma_{2D}/\lambda$.

(U) A computer simulation program was used in the course of the present effort to calculate the normalized RCS, $B = \sigma/L^2$, of numerous camouflaged-edge configurations as functions of aspect. The simulation program used the Method of Moments, which is based on the following point of view: a wave, generated by the radar and incident on the scatterer, induces currents on the scatterer. The excited scatterer then reradiates energy, some of it back in the direction of the radar.

(U) Representation of the scatterer is strictly 2-D, at a single radar frequency, with the geometry of the scatterer represented numerically in terms of a finite number of points in a plane. As a rule of thumb, these points should be at most a tenth of a radar wavelength apart.

(U) Applicablity of the computer program was limited to radars polarized parallel to the camouflaged edge (E-polarization), illuminating:

- Metal bodies

- Thin, electrically lossy sheets

- Dielectric bodies

(U) Special features of the program, developed especially for the present effort, include:

- Maximum-speed subroutines at critical high-repetition locations in the program to reduce to a minimum the computer time needed to generate an electromagnetic representation of the scattering body.

- Double-precision accumulation of critical totals, to preserve numerical accuracy at low-RCS aspects.

- High-efficiency engineering-trial algorithm, making it possible to modify the electrical parameters of edge treatments with a bare minimum of new computatation.

(U) These features deserve special comment. The engineering-trial algorithm made it practical to engage in well over a hundred trial selections of electrical parameter values in efforts to electrically optimize several geometrical designs for edge treatments. Even with the penalty accompanying the conversion to double precision, the three special features reduced the computer time used in the edge-treatment optimization by an order of magnitude.

(U) <u>Multiple Testing Feature</u> - This technical discussion discloses the mathematical advance that made it practical to test numerous edge-treatment candidates in a small fraction of the computer time required heretofore. It is based on the concept that the edge treatment is all that changes from trial to trial, and so it is best to invert a large matrix (representing the treated body along with the treatment) only once in a set-up step and then, once for each successive trial, invert a much smaller matrix (representing only the treatment itself.

(U) The basic E-polarization integral equation to be solved is

$$Z_s(x,y)\, j(x,y) \;+\; \int_C Z\!\left(k\left[(x'-x)^2 + (y'-y)^2\right]^{1/2}\right) j(x',y')\, ds' \;=\; e^{inc}(x,y)$$

where (x,y) are the coordinates of the points on C, which consist of the boundary of the treated metal body together with infinitely thin sheets of impedance Z_s. The Z-component of the induced current is j and of the incident electric field is e^{inc}. The kernel is expressed in SI units in ohms/meter and is given by $Z = -(\omega\mu_0/4)\, H_0^{(1)}$ where $H_0^{(1)}$ is the Hankel function of the first kind of order zero, and $k = 2\pi/\lambda$.

(U) The basic integral equation can be written in matrix form as

$$\left[Z_s + Z\right] j \;=\; \left[\Delta Z_s + K\right] j \;=\; e^{inc}$$

(U) The change of sheet impedance Z_s from the "base case" value Z_{s0} is ΔZ_s. Let

$$\Delta Z_s \;=\; \begin{pmatrix} z & 0 \\ 0 & 0 \end{pmatrix}$$

and let

$$K^{-1} \;=\; \begin{pmatrix} A & B \\ C & D \end{pmatrix}$$

where z and A are $M \times M$ matrices, $M < N$. Then, rewriting the basic equation as

$$\left[K^{-1}\, \Delta Z_s + I_N\right] j \;=\; K^{-1}\, e^{inc}$$

and partitioning (here I_N is the $N \times N$ identity matrix), we have

$$\left[\begin{pmatrix} A & B \\ C & D \end{pmatrix}\begin{pmatrix} z & 0 \\ 0 & 0 \end{pmatrix} + \begin{pmatrix} I_M & 0 \\ 0 & I_{N-M} \end{pmatrix}\right]\begin{pmatrix} j_M \\ j_{N-M} \end{pmatrix} = \begin{pmatrix} A & B \\ C & D \end{pmatrix} e^{inc} = \begin{pmatrix} r \\ s \end{pmatrix}$$

Thus, we find

$$j_M = (Az + 1_M)^{-1} r \qquad \text{and} \qquad j_{N-M} = s - Czj_M$$

which solves the problem.

(U) The technique reported here was developed for conveniently measuring $B = \sigma/L^2$ of candidate treated edge configurations in order (1) to provide data under conditions beyond the capability of computer simulation; (2) to test the validity of computer simulations; and (3) to test physical realizations of theoretical edge-treatment designs.

(U) <u>Test Object</u> - The ideal 3-D treated-edge test object, described in terms of a 2-D figure on the xy-plane, extends to infinity in the +z, -z and +x-directions.

(U) <u>Materials</u> - Ideally, lossy dielectric materials should be available, made to order with specified complex magnetic and electric constitutive parameters μ and ϵ.

(U) <u>RCS Test Range</u> - Ideally, the test range should be quite free of background backscatter. (For further discussion, see the last two pages of Section 2.0.)

(U) <u>Test Object</u> - Almost all metal edges tested in the present effort were modeled on an aluminum object like the one shown in Figures 21 and 22. Design features of this simple test object were the following: its treated edge was approximately three wavelengths long, for an effectively uniform edge-current distribution; its ends were flat so that the object would stand on end; and its untreated edge was canted 30 degrees to reduce interference with the treated edge by at least 9 decibels.

(U) <u>Materials</u> - Spaced, thin resistive sheets simulated lossy dielectrics having relative complex dielectric constants of the form 1 + a - ia. Carbon-loaded flexible polyurethane foam was available made to order, but tight quality control was prohibitive.

(U) A typical edge-camouflage test set-up is shown in Figure 21, together with resultant data for E-polarization (electric field vector parallel to the treated edge). Figure 22 shows how a rough assessment can be made of the level of background contributed by the test object. The graph plotted in Figure 23 gives the maximum decibel error due to the presence of background.
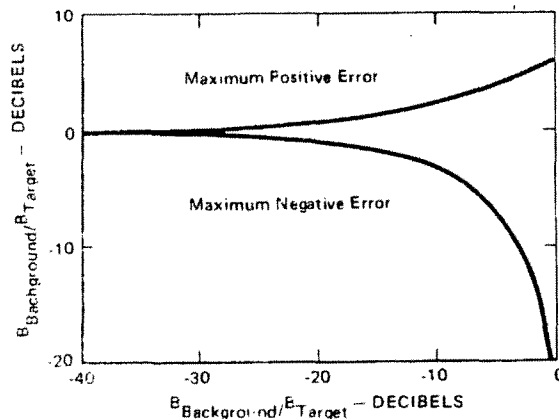
(U)   Figure 23. Maximum Decibel Errors in Measurements of $B = \sigma/L^2$
                        Due to Background

(U) The edge treatment chosen for the low-RCS demonstration vehicle resulted from an extensive exploration of candidate designs and design concepts, based on work at Teledyne Ryan Aeronautical (TRA) dating back to 1967.

(U) Summary of Effort – An intensive effort to optimize the previously developed edge treatment designs resulted in the layered-dielectric design installed on the 1/3-scale model of the low-RCS demonstration vehicle.

(U) It seems reasonable to expect that a new bulk-dielectric edge treatment, designed with the aid of computer simulation and fabricated in a one-piece, unlayered physical realization (Paragraph 3.4) would exhibit performance quite superior to that of any built heretofore.

(U) RAM-based design approach. A layer of radar absorbing material camouflages a reflecting metal surface (Paragraph 3.1) by attenuating an incident radar wave on its way to the metal surface, and then further attenuating the wave on its way back out. The attenuating layer functions by absorbing energy from the wave and dissipating it as heat. To a first approximation, the problem in RAM-panel design is to camouflage the reflection from the front surface of the attenuating layer. This is done by placing a second, less strongly attenuating layer in front of the inner layer and continuing with additional layers until the desired degree of camouflage is achieved.

Computer Simulation – The edge treatment used on the 1/3-scale demonstration model is based on the sheet-impedance distribution whose absolute magnitude is graphed in Figure 29. The phase angle of the sheet impedance is 45 degrees capacitive. The computer simulation geometry is shown in Figure 30 to the same scale as the graph of the impedance distribution above and the graph of current distribution in Figure 31.
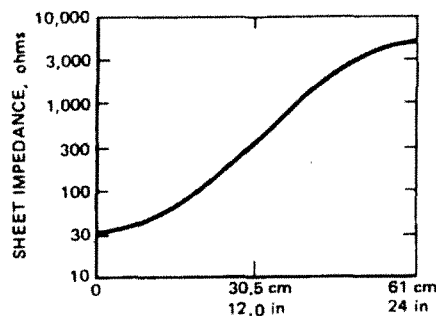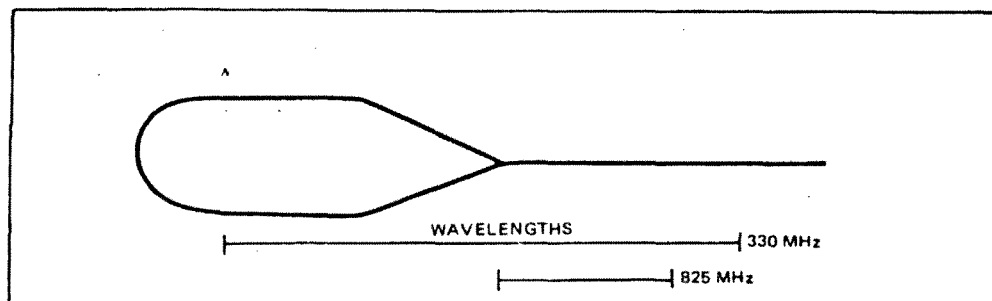

Figure 29. Sheet Impedance Distribution

Figure 30. Simulation Geometry for Single-Sheet Treatment of Sharp Metal Edge
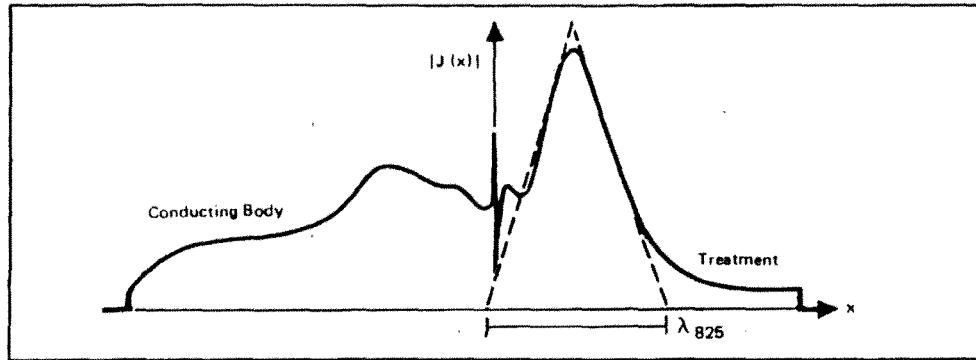
Figure 31. Distribution of Effective Induced Current Density

(U)

(U) <u>Measured Performance</u> – Information on the leading-edge treatment of the 1/3-scale model was presented in Table 4. Corresponding information is presented in Figure 34 for frequencies at which each trailing edge is at least long enough for the two trailing edge lobes to backscatter independently (to within the accuracy of the measurements).

(U) <u>A Summing Up</u> – Science and technology advance by a continual leap-frogging of theory and experiment. In the present instance, a fund of experimental data existed from previous programs. The edge-treatment optimization effort began with a theoretical preparation for further experimentation. The experimentation that followed led to the design of the demonstration edge-treatment responsible, in part, for the hundredfold advance in the state of the radar-camouflage art reported in Section 2.0. Moreover, this experimentation set the stage for further theoretical developments which have been initiated and which show great promise.

(U) The multidisciplinary approach used in the design of the high-altitude reconnaissance vehicle of Section 2.0 is readily applicable to other types of military aircraft as well. Three types of aircraft are mentioned below as examples of the generality of the approach.

(U) As mentioned in Section 1.0, radar camouflage is used in warfare to deny to the enemy:

- Detection of our aircraft
- Tracking of our aircraft
- Fuzing of his weapons launched against our aircraft

(U) A high-altitude penetrator capable of escaping detection (and tracking and fuzing as well, of course), would probably resemble the vehicle of Section 2.0 very closely. That is, it would probably be a delta flying wing without fuselage. But aircraft designed for other flight regimes and tactical environments might well look quite different.

(U) A low-altitude penetrator could easily be a double delta similar in design to the SR-71. Flying low, it might be detected easily particularly by non-radar means, but its inherently low microwave RCS would protect it from tracking radars and radar-fuzed missiles.

(U) The effectiveness of the multidisciplinary approach lies in its ability to foster the application of the first rule, as well as the second. Notice that these rules are quite compatible with supersonic as well as subsonic design.

(U) The present discussion is a brief recapitulation of the one presented in Paragraph 1.3. It summarizes the requirements and limitations of camouflage to deny to the enemy detection, tracking, and fuzing.

(U) Denial of Detection - Three considerations are paramount here:

1. The camouflage must be effective across the entire threat radar spectrum, from 100 MHz or less to 10 GHz.

2. A low RCS is the only countermeasure available to combat detection.

3. Camouflage against detection is a threshold effect. There is no use in reducing the RCS of an aircraft if it cannot be reduced to the level necessary to hide the aircraft.

(U) Denial of Tracking - Contrasted with the three considerations listed above, we have the following:

1. The camouflage must be effective only across the spectrum of threat tracking radars, from 900 MHz or slightly less, to 10 GHz or somewhat more.

2. Chaff and active electronic countermeasures (ECM), such as jamming, are available to use against trackers.

3. Any reduction in RCS increases the effectiveness of chaff and active ECM, and correspondingly reduces the necessary weight and power penalties that their use entails.

(U) Denial of Fuzing - Like camouflage against detection, camouflage against fuzing is a threshold effect. The camouflage really becomes effective only when it reduces the fuzing radius of a threat weapon below its CEP. As noted in Figure 3, if the fuzing radius of a weapon fired at a low-RCS aircraft is 40 percent of its CEP, the single-shot kill probability of the weapon drops to only 10 percent.

(U) The Low-RCS Demonstration Vehicle of Section 2.0 is an example of a high-altitude penetrator, a type of vehicle that is able to benefit greatly from radar camouflage against detection as well as against tracking and fuzing.

(U) The data plotted in Figure 36 summarize the aerodynamic performance of a family of high-altitude penetrators, including as a special case the Low-RCS Demonstration Vehicle of Section 2.0. Like other aircraft concepts, the penetrator discussed on the previous pages, and illustrated in Figure 6 can be applied to a wide range of mission and performance requirements, with the size of the vehicle dependent on choice of power plant, payload, and particular mission requirements.

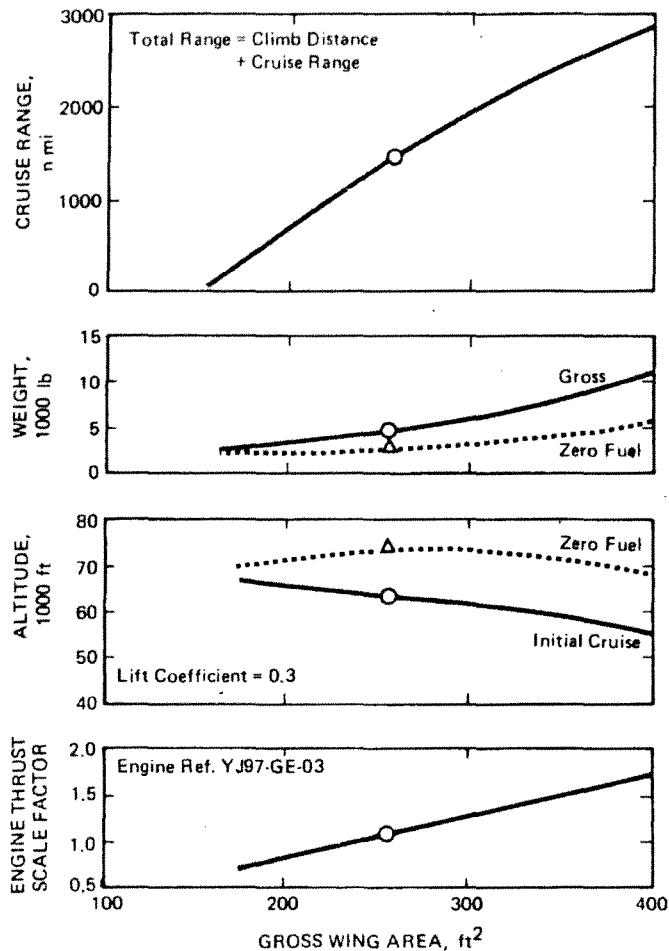| Aspect Ratio:	2.5
Edge-Treatment Width:	24 in
Payload:	400 lb
Maximum Lift/Drag:	10.5
Climb Distance:	85 n mi
Cruise Mach:	0.8

Figure 36. High Altitude Penetrator Performance as a Function of Gross Wing Area.
Note Performance Values for the 260 ft^2 Low-RCS Demonstration Vehicle.

(U)

(U) As in the case of the Low-Altitude Penetrator, opposite, the low-altitude mission of the mini-RPV requires only microwave camouflage to deny to the enemy tracking and fuzing. With regard to detection, survivability, not surprise, is of prime importance. Indeed, in a decoy role, it might even be desirable and cost-effective to draw enemy fire if the chances for a hit are very, very small.

(U) The preceding examples show three products of a multidisplinary team charged with the design of aircraft, each having aerodynamic performance optimized for its particular type of mission and having an inherently low degree of radar reflectivity as well. By adhering to the two basic rules discussed below, the team has designed aircraft having good aerodynamic-performance characteristics, and radar-camouflage characteristics radically improved over those of conventional radar-camouflaged designs (for example, Figure 4).

(U) Building on the advances reported here, the Air Force Laboratories should further develop the technology needed to facilitate the design of aircraft capable of meeting Air Force requirements for low observables. These requirements were often compromised in the past, owing to the absence of such technology. Already, however, exploitation of the multidisciplinary design approach disclosed here has resulted in a low-RCS mini-RPV, under development and due to fly in early 1975. This mini-RPV was designed in accordance with the three-part concept outlined on the opposite page. It is without edge treatment, however, owing in part to the current underdeveloped state of edge-treatment technology.

(U) Edge-treatment technology needs to be brought to the same high state of development to which the Air Force Laboratories have brought radar absorbing material panel technology. Accordingly, a five-prong technology-development effort is recommended in the areas of theory, computer simulation, experimental measurement, fabrication, and materials. Specific Air Force needs in these areas are listed below.

(U) Simulation - High-efficiency, multiple-trial computer programs are needed, capable of accommodating incident radar waves of arbitrary polarizations.

(U) Experimental Measurement - Metal-edged test objects are needed whose RCS' are 1/100 those of existing test objects (exclusive of the metal test edges themselves) and yet are simple to build and easy to use. Moreover, test-model support technology also needs further development to reduce the RCS contributions of the model supports themselves.

(U) Fabrication - Methods are needed for fabricating edge treatments with a minimum number of joints, of minimum reflectivity.

(U) Materials - Rigid, strong, easily worked dielectric and magnetic materials are needed, with uniform, reproducible electromagnetic properties.

(U) Timely development of technologies in these areas is necessary to the full, efficient application of the multidisciplinary approach to current and future Air Force needs for low-observables and, in particular, low-RCS aircraft.